Petroleum Science and Engineering
2026, Vol. 10, No. 2, pp. 115–129
https://doi.org/10.11648/j.pse.20261002.14

SciencePG
Science Publishing Group

Research Article

Validation of an LSDF-Adjusted Inspection Framework for Pipeline Maintenance Planning in the Niger Delta

Utiri Collins David[1, *], **Elizabeth Chinyerem Ndubuisi**[2]

[1]Institute of Engineering, Technology and Innovation Management (METI), University of Port Harcourt, Port Harcourt, Nigeria

[2]Department of Petroleum and Gas Engineering, University of Port Harcourt, Port Harcourt, Nigeria

Abstract

Static inspection programmes may apply uniform inspection intervals across heterogeneous asset populations, whereas risk-based inspection (RBI) seeks to differentiate inspection priorities according to assessed risk. However, location-specific environmental, biological and socio-security exposure is not always represented explicitly in inspection scheduling. This study evaluates and internally validates a Location-Specific Degradation Factor (LSDF) as a decision-support layer for inspection planning across twelve Niger Delta pipeline locations. LSDF scores were converted to an effective corrosion rate using the calibrated amplification model $CR_{eff}=CR_{base}$ (1+k· LSDF), with k≈4.74 estimated by root-mean-square error (RMSE) minimisation, and subsequently mapped to LSDF severity classes and study-specific maximum inspection intervals. In-sample predicted-versus-observed degradation rates showed strong agreement (Pearson r=0.998, predictive R^2=0.993, RMSE = 0.064 mm/yr, and classification accuracy = 91.7%, 11/12; exact 95% confidence interval (CI): 61.5-99.8%). Leave-one-location-out cross-validation (LOLO-CV) preserved classification accuracy at 91.7% (11/12; exact 95% CI: 61.5-99.8%) while giving a more conservative RMSE of 0.073 mm/yr, and stable refitted k values of 4.710-4.804. Relative to a uniform 36-month static inspection benchmark, the LSDF-based policy assigned shorter inspection intervals to locations with greater degradation exposure and longer intervals to locations with lower exposure. This reallocation increased total scheduled inspection events over five years from 24 to 62 (+158.3%), reflecting intensified surveillance of higher-severity locations rather than an overall reduction in inspection activity. No economic-benefit claim is made because location-specific inspection, mobilisation, failure-consequence and discount-rate data were unavailable. The LSDF is therefore proposed as a location-sensitive decision-support layer that complements, rather than replaces, established RBI and condition-based integrity assessment.

Keywords

Risk-based Inspection, Pipeline Corrosion, Predictive Maintenance, Cross-validation, Niger Delta, Asset Integrity

1. Introduction

Location-specific degradation severity becomes practically useful for pipeline integrity management when it can be translated into differentiated inspection or maintenance decisions. In the Niger Delta, pipeline assets traverse coastal

*Correspondence: Utiri Collins David (collins_utiri@uniport.edu.ng)

Received: 26 September 2026; **Accepted:** 9 October 2026; **Published:** 12 November 2026

Copyright: © The Author(s), 2026. Published by Science Publishing Group. This is an **Open Access** article, distributed under the terms of the Creative Commons Attribution 4.0 License (http://creativecommons.org/licenses/by/4.0/), which permits unrestricted use, distribution and reproduction in any medium, provided the original work is properly cited.

mangrove, transitional swamp and inland upland-fringe environments that differ substantially in climatic, environmental, biological and socio-security exposure. To represent this spatial heterogeneity quantitatively, the present study employs a Location-Specific Degradation Factor (LSDF), formulated as an Analytic Hierarchy Process (AHP)-weighted composite index integrating nine screened environmental, biological and socio-security variables into a single location-specific exposure-severity score. The AHP weighting procedure produced an internally consistent comparison matrix (λ_{max} = 9.1455, consistency ratio (CR) = 0.013), with flood frequency receiving the highest weight (25.4%), followed by salinity, soil-corrosivity score and vandalism frequency (15.9% each). Across the twelve analysed pipeline locations (A-L), LSDF values ranged from 0.000 to 1.000, reflecting substantial spatial variation in degradation exposure.

The operational question addressed in this study is whether incorporation of location-specific degradation exposure into inspection planning can support more differentiated inspection intervals than a uniform static schedule. The proposed decision pathway is:

Location exposure→LSDF→CReff→LSDF severity class→inspection interval

where CR_{eff} represents the LSDF-adjusted effective corrosion rate. Contemporary risk-based inspection (RBI) practice, formalised in American Petroleum Institute (API) Recommended Practice (RP) 580 and API RP 581 [1, 2] and increasingly characterised by performance-based and data-driven decision approaches [3, 4], provides the broader integrity-management context within which this location-sensitive exposure layer is intended to operate. The LSDF is therefore conceived as a decision-support layer that complements, rather than replaces, condition-based inspection data, probability- and consequence-based risk assessment, fitness-for-service evaluation and engineering judgement.

The relevance of incorporating location-specific exposure is particularly pronounced in the Niger Delta, where pipeline integrity is influenced not only by environmental and corrosion-related processes but also by substantial third-party interference. Nigeria recorded more than 589 reported oil spills in 2024, with a large proportion attributed to oil theft and sabotage rather than equipment failure, according to National Oil Spill Detection and Response Agency (NOSDRA) data [5]; attitudes toward pipeline vandalism in oil-producing communities are also shaped by local socio-economic conditions [6]. Such conditions indicate that socio-security exposure can materially influence integrity-management requirements and should not necessarily be treated as peripheral to inspection planning.

Against this background, the study evaluates the complete LSDF-to-inspection decision pathway by calibrating an effective corrosion-rate model, comparing predicted and observed degradation rates, assessing predictive stability through leave-one-location-out cross-validation (LOLO-CV), examining terrain-specific performance, and comparing the resulting inspection policy with a uniform 36-month static inspection benchmark. The analysis also reconciles inspection-event counts over a five-year planning horizon. Economic performance is treated separately from technical validation because the available dataset does not contain the complete inspection, mobilisation, failure-consequence and discount-rate information required for a defensible net present value (NPV), return on investment (ROI) or payback analysis.

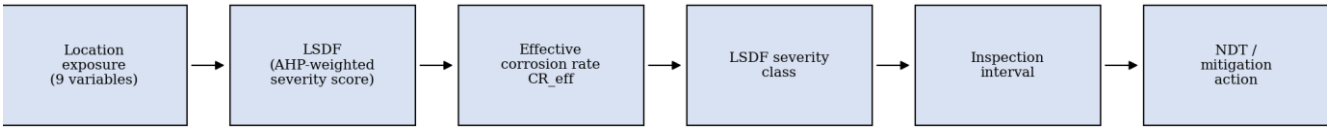


Figure 1. *LSDF-to-RBI decision-logic architecture: location exposure is translated sequentially into a maintenance/inspection decision.*

2. Materials and Methods

2.1. LSDF Formulation and Model Inputs

The Location-Specific Degradation Factor (LSDF) was formulated as an AHP-weighted composite index representing relative environmental, biological and socio-security exposure at each pipeline location. Nine variables, retained after collinearity screening [7], were included: rainfall, humidity, salinity, flood frequency, soil-corrosivity score, microbiologically influenced corrosion (MIC) activity score, wetland exposure, vandalism frequency and accessibility-related exposure score. MIC activity was included because microbial processes are an established contributor to the degradation of steel pipelines [8, 9]. Each variable was transformed to a common dimensionless scale using min-max normalisation, and the LSDF for location i was calculated as

$$LSDF_i = \Sigma_{j=1}^{9} w_j X_{ij}^* \quad (1)$$

where X_{ij}^* is the normalised value of variable j at location i, and w_j is its corresponding AHP-derived weight, subject to $\Sigma_{j=1}^{9} w_j = 1$ and $0 \leq LSDF_i \leq 1$.

The criterion weights were derived from the principal ei-

genvector of an aggregated reciprocal AHP pairwise-comparison matrix, an approach also applied in recent importance and risk assessment of pipeline facilities [10]. The resulting weight structure assigned the highest priority to flood frequency (0.2541), followed by salinity (0.1586), soil-corrosivity score (0.1586), vandalism frequency (0.1586), MIC-activity score (0.0984), rainfall (0.0633), humidity (0.0405), wetland exposure (0.0404) and accessibility-related exposure score (0.0275). The aggregated matrix yielded λ_{max}=9.1455 and a consistency ratio of CR=0.013, indicating acceptable internal consistency of the AHP judgements.

The resulting location-specific LSDF values were treated as fixed exposure-severity inputs in the present inspection-planning analysis. They were not re-estimated during calibration of the corrosion-rate amplification coefficient k. This separation preserves the distinction between the AHP-based exposure model and the subsequent calibration of the effective corrosion-rate relationship. The LSDF values and other essential model inputs used in the analysis are presented in Table 1.

Table 1. *Final LSDF values and essential model inputs (baseline corrosion rate, calibrated amplification coefficient).*

Location	LSDF	CR_{base} (mm/yr)	Calibrated k
A	1.000	0.50	4.74
B	0.874	0.50	4.74
C	0.929	0.50	4.74
D	0.791	0.50	4.74
E	0.632	0.50	4.74
F	0.580	0.50	4.74
G	0.510	0.50	4.74
H	0.450	0.50	4.74
I	0.169	0.50	4.74
J	0.123	0.50	4.74
K	0.044	0.50	4.74
L	0.000	0.50	4.74

LSDF values were obtained from the LSDF formulation described in Section 2.1. The baseline corrosion rate, CR_{base}, and calibrated amplification coefficient, k, are defined in Section 2.2 and summarised in Table 2.

2.2. Baseline and Effective Corrosion Rate

A common reference baseline corrosion rate of 0.50 mm/yr was adopted for all twelve study locations:

$$CR_{base}=0.50 \text{ mm/yr} \quad (2)$$

The value was treated as a common modelling baseline rather than as a location-specific measured corrosion rate. Detailed metadata describing the individual inspections, observation period, wall-thickness basis or derivation of this reference value were not retained in the archived analytical dataset. Accordingly, CR_{base} is used solely as the reference deterioration rate prior to location-specific adjustment, and this limitation is acknowledged in Section 4.3. The baseline corrosion rate is independent of the LSDF and is not interpreted as being caused by location-specific exposure.

The LSDF-adjusted effective corrosion rate for location i was defined as

$$CR_{eff,I}=CR_{base}\,(1+k\,LSDF_i) \quad (3)$$

where $CR_{eff,I}$ is the predicted effective corrosion rate, $LSDF_i$ is the Location-Specific Degradation Factor for location i, and k is an empirically calibrated amplification coefficient. The formulation satisfies the boundary condition $CR_{eff,i}=CR_{base}$ when $LSDF_i=0$, while allowing the predicted degradation rate to increase progressively with location-specific exposure severity. The parameter k is therefore a calibration coefficient and is distinct from the AHP-derived criterion weights used in constructing the LSDF. Recent data-driven studies have likewise related environmental variables such as salinity, moisture and carbon dioxide (CO_2) partial pressure to the corrosion rate of pipeline steels [11, 12]; the single-parameter linear form adopted here is deliberately parsimonious given the twelve-location sample.

The value of k was estimated by minimising the root-mean-

square error (RMSE) between predicted effective corrosion rates and observed annual degradation rates (ADR):

$$RMSE(k) = \sqrt{\frac{1}{n_c}\sum_{i=1}^{n_c}(CR_{pred,i}(k) - ADR_i)^2} \quad (4)$$

where $CR_{pred,I}(k)$ is the model-predicted corrosion rate for a specified value of k, ADR_i is the observed annual degradation rate at location i, and n_c is the number of observations used in calibration.

The calibrated amplification coefficient was k≈4.74. At Location A, where LSDF=1.000, the resulting effective corrosion rate was 2.87 mm/yr, equivalent to approximately 5.7 times the adopted baseline value. The stability of the calibration coefficient was subsequently examined using leave-one-location-out cross-validation, which produced refitted k values ranging from 4.710 to 4.804 (Section 3.3).

Table 2. *Calibration and validation characteristics of the LSDF effective corrosion-rate model.*

Parameter / performance measure	Value
Functional form	$CR_{eff}=CR_{base}(1+k\cdot LSDF)$
Baseline corrosion rate, CR_{base}	0.50 mm/yr
Calibration method	RMSE minimisation
Calibrated amplification coefficient, k	4.74
LOLO-CV refitted k range	4.710-4.804
Predictive R^2	0.993
RMSE	0.064 mm/yr
MAE	0.055 mm/yr
MAPE	4.0%
LOLO-CV RMSE	0.073 mm/yr

LOLO-CV: leave-one-location-out cross-validation; MAE: mean absolute error; MAPE: mean absolute percentage error; RMSE: root-mean-square error.

Table note: The linear amplification model was the evaluated functional form used throughout the present analysis. Model performance was assessed using predicted-versus-observed degradation rates and leave-one-location-out cross-validation.

Table 3 reports the resulting effective corrosion rate, $CR_{eff} = CR_{base}(1+k \cdot LSDF)$, for all twelve locations using the calibrated linear model.

Table 3. *Effective corrosion rate (CR_{eff}) for all twelve locations (linear model, k=4.74).*

Location	LSDF	CR_{base} (mm/yr)	CR_{eff} (mm/yr)
A	1.000	0.50	2.87
B	0.874	0.50	2.57
C	0.929	0.50	2.70
D	0.791	0.50	2.38
E	0.632	0.50	2.00
F	0.580	0.50	1.87
G	0.510	0.50	1.71
H	0.450	0.50	1.57
I	0.169	0.50	0.90

Location	LSDF	CR_{base} (mm/yr)	CR_{eff} (mm/yr)
J	0.123	0.50	0.79
K	0.044	0.50	0.61
L	0.000	0.50	0.50

2.3. LSDF Severity Classification and Inspection-Interval Decision Matrix

Each LSDF score was mapped to a severity class and study-specific maximum inspection interval using the decision matrix presented in Table 4. The matrix also specifies effective-corrosion-rate ranges used independently to classify observed annual degradation rates (ADR) for validation (Section 3.2), so that predicted (LSDF-derived) and observed (ADR-derived) classes are obtained from two distinct inputs rather than the same one. The five LSDF severity bands are defined over the 0-1 LSDF scale, while the corresponding effective-corrosion-rate ranges constitute study-specific classification thresholds used to assign observed ADR severity classes. The LSDF severity thresholds, effective-corrosion-rate thresholds and inspection intervals are study-specific decision rules adopted for framework evaluation; they have not been externally validated as universally applicable thresholds or inspection frequencies.

Table 4. *LSDF severity class - effective-corrosion-rate range - inspection interval - NDT decision matrix.*

LSDF range	LSDF severity class	Effective corrosion rate range (mm/yr)	Maximum interval	Indicative NDT / inspection
0.81-1.00	Critical	> 2.5	≤6 months	ILI/MFL+UT, PAUT, ECDA
0.61-0.80	High	1.8 - 2.5	≤12 months	PAUT, UT mapping
0.41-0.60	Moderate	1.2 - 1.8	≤24 months	UT grid / corrosion monitoring
0.21-0.40	Low	0.8 - 1.2	≤36 months	Visual inspection / periodic UT
0.00-0.20	Very Low	< 0.8	≤60 months	Visual inspection / UT spot checks

NDT: non-destructive testing; ILI: in-line inspection; MFL: magnetic flux leakage; UT: ultrasonic testing; PAUT: phased-array ultrasonic testing; ECDA: external corrosion direct assessment. This decision matrix specifies study-specific maximum inspection intervals and LSDF severity thresholds. It is intended as a decision-support framework for the present analysis and does not replace established RBI procedures, fitness-for-service assessment, engineering judgement, or applicable regulatory requirements. The intervals have not been independently validated as universally applicable inspection frequencies.

2.4. Calibration/Validation Separation and Cross-validation

Because n=12 is small, calibration and validation roles were kept conceptually distinct: development data established variable transformation and model structure; calibration data were used to estimate k; and a model component was not calibrated against observations subsequently presented as independent validation. Where a conventional fixed split was impractical at this sample size, LOLO-CV was used: for each location i in turn, i was withheld, k was re-estimated from the remaining eleven locations, the withheld location's CR_{eff} was predicted using that refit k, and the prediction error and LSDF severity classification were recorded. LSDF is an input to this procedure, not a withheld prediction; the quantity actually predicted out-of-fold is the effective corrosion rate, so the cross-validation error is defined as

$$e_i^{LOLO} = CR_{eff,i}^{(-i)} - ADR_i \quad (5)$$

where $CR_{eff,i}^{(-i)}$ is the effective-corrosion-rate prediction for location i obtained using k refit from the other eleven locations, and ADR_i is the observed annual degradation rate at location i. LOLO performance was summarised using mean absolute error (MAE), RMSE, maximum absolute error and classification accuracy, reported separately from the in-sample (apparent) fit statistics (Section 3.3), consistent with general guidance that leave-one-out-style estimators require separate reporting from apparent performance and can carry non-trivial

bias in small samples [13].

2.5. Validation Metrics

Predicted ($P_i = CR_{eff,i}$) and observed ($O_i = ADR_i$) degradation rates were compared using Pearson correlation,

$$r = \frac{\sum_{i=1}^{n}(P_i - \bar{P})(O_i - \bar{O})}{\sqrt{\sum_{i=1}^{n}(P_i - \bar{P})^2 \sum_{i=1}^{n}(O_i - \bar{O})^2}} \quad (6)$$

Spearman rank correlation ρ (as a non-parametric, linearity-free check on rank preservation), and the predictive coefficient of determination, calculated as

$$R^2 = 1 - \frac{\sum_{i=1}^{n}(O_i - P_i)^2}{\sum_{i=1}^{n}(O_i - \bar{O})^2} \quad (7)$$

which compares predictions directly against the observed mean and is not necessarily identical to the r^2 of an ordinary least-squares regression of predicted on observed values; the reported value (Section 3.2) is this predictive R^2, consistent with the acceptance criterion below. The prediction-error metrics were

$$RMSE = \sqrt{\frac{1}{n}\sum_{i=1}^{n}(P_i - O_i)^2} \quad (8)$$

$$MAE = \frac{1}{n}\sum_{i=1}^{n}|P_i - O_i| \quad (9)$$

$$MAPE = \frac{100}{n}\sum_{i=1}^{n}\left|\frac{P_i - O_i}{O_i}\right| \quad (10)$$

Pre-specified acceptance criteria were RMSE ≤ 20% of mean observed ADR, MAE ≤ 15% of mean observed ADR, and mean absolute percentage error (MAPE) ≤ 10%. Predicted and observed LSDF severity classes were additionally cross-tabulated in a confusion matrix (Section 3.2) the observed class was assigned from the observed ADR using the effective-corrosion-rate ranges of Table 4, independently of the LSDF-derived predicted class from which per-class precision, recall and F1 were computed as

$$Precision_c = \frac{TP_c}{TP_c + FP_c} \quad (11)$$

$$Recall_c = \frac{TP_c}{TP_c + FN_c} \quad (12)$$

$$F1_c = 2\frac{Precision_c \times Recall_c}{Precision_c + Recall_c} \quad (13)$$

with macro-averaged performance summarised as:

$$Macro\text{-}F1 = \frac{1}{C}\sum_{c=1}^{C} F1_c,$$

$$Balanced\ Accuracy = \frac{1}{C}\sum_{c=1}^{C} Recall_c \quad (14)$$

where TP_c, FP_c and FN_c are the numbers of true positives (TP), false positives (FP) and false negatives (FN) for severity class c, $F1_c$ is the F1-score (the harmonic mean of precision and recall) for class c, and C is the number of severity classes.

The 95% confidence interval (CI) for classification accuracy was estimated using an exact (Clopper-Pearson) binomial procedure rather than a large-sample normal approximation, reflecting the small (n=12) validation sample; the resulting intervals, reported in Sections 3.2 and 3.3, are wide, which honestly reflects the sampling uncertainty inherent in n=12.

2.6. Comparison with a Uniform 36-month Benchmark Schedule

The uniform 36-month static inspection benchmark was defined as a fixed 36-month inspection interval applied to all twelve locations, identical in asset population and analysis horizon to the LSDF-adjusted condition. For each location, the interval difference and percentage change relative to the LSDF-prescribed interval were:

$$\Delta I_i = I_{conventional,i} - I_{LSDF,i} \quad (15)$$

$$\%\Delta I_i = \frac{I_{LSDF,i} - I_{contentional,i}}{I_{conventional,i}} \times 100 \quad (16)$$

The number of scheduled inspection events over a five-year analysis horizon T was calculated from the assigned interval, using the counting convention

$$N_i = \left[\frac{T}{I_i}\right] \quad (17)$$

where T is the five-year analysis horizon and I_i is the assigned inspection interval, with the initial inspection counted at t=0. The same convention was applied identically to both the uniform benchmark and LSDF-adjusted schedules. Because the LSDF-prescribed interval is obtained directly from the LSDF decision matrix (Table 4) and the benchmark is compared against that same LSDF-prescribed interval, this comparison quantifies how the LSDF policy reallocates inspection frequency relative to an external uniform benchmark; it is a policy-comparison analysis, not an independent validation of the LSDF-derived inspection intervals, since the LSDF interval is not itself independently derived in this comparison. A location was classified as over-scheduled relative to the LSDF policy when the benchmark assigned a shorter interval (more frequent inspection) than the LSDF policy prescribed, and under-scheduled relative to the LSDF policy when the benchmark assigned a longer interval (less frequent inspection) than prescribed; these are directly countable event-frequency comparisons and are not presented as diagnostic accuracy or classification-error rates.

Because this study reports inspection-event arithmetic only, and unit inspection cost, mobilisation cost, monitoring cost, avoided-failure benefit and discount rate were not available

for the twelve-location dataset, a full life-cycle economic (NPV/ROI/payback) model was not developed; this limitation is carried through explicitly into Section 3.5 and Section 4.1 rather than resolved by assumption.

3. Results

3.1. Predicted Versus Observed Effective Corrosion Rate

Table 5 reports the predicted effective corrosion rate (from Table 3) and observed annual degradation rate (ADR) for all twelve locations, together with the prediction residual.

Table 5. *Predicted versus observed degradation: effective corrosion rate versus observed ADR, by location.*

Location	LSDF	Predicted CR_{eff} (mm/yr)	Observed ADR (mm/yr)	Residual (mm/yr)
A	1.000	2.87	2.76	+0.11
B	0.874	2.57	2.51	+0.06
C	0.929	2.70	2.68	+0.02
D	0.791	2.38	2.42	−0.04
E	0.632	2.00	2.10	−0.10
F	0.580	1.87	1.96	−0.09
G	0.510	1.71	1.72	−0.01
H	0.450	1.57	1.61	−0.04
I	0.169	0.90	0.89	+0.01
J	0.123	0.79	0.84	−0.05
K	0.044	0.61	0.69	−0.08
L	0.000	0.50	0.54	−0.04

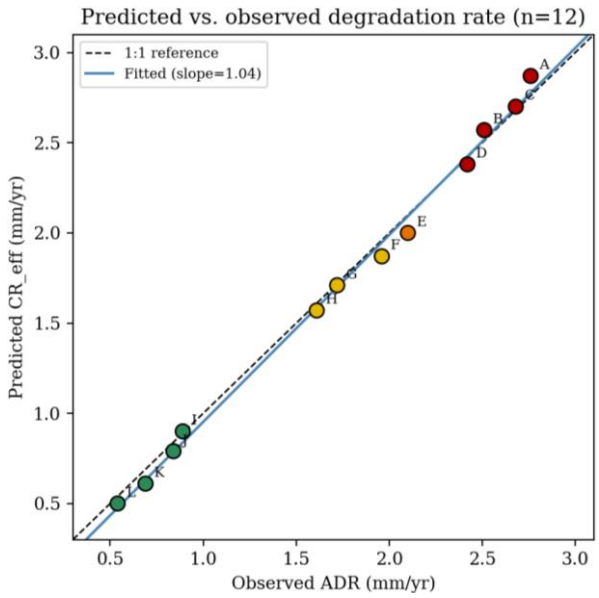


Figure 2. *Predicted effective corrosion rate versus observed ADR (n=12), with 1: 1 reference and fitted line.*

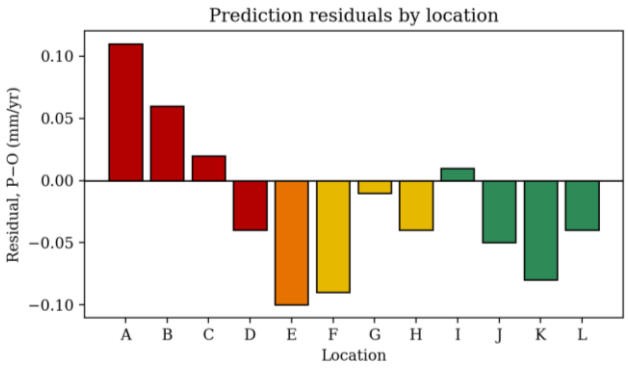


Figure 3. *Prediction residuals by location.*

3.2. Validation Performance and Severity-classification Accuracy

Table 6 presents the principal in-sample validation metrics for the twelve-location dataset, comprising Pearson correlation (r), Spearman rank correlation (ρ), predictive R^2, root-mean-square error (RMSE), mean absolute error (MAE),

mean absolute percentage error (MAPE), and severity-classification accuracy.

Table 6. *In-sample validation performance of the LSDF-adjusted effective corrosion-rate model (n = 12).*

Metric	Computed value	Acceptance threshold	Assessment
Pearson correlation, r	0.998	≥ 0.80	Very strong positive association
Spearman rank correlation, ρ	1.000	≥ 0.70	Complete rank agreement
Predictive R^2	0.993	≥ 0.65	Exceeds threshold
RMSE	0.064 mm/yr	≤ 20% of mean ADR	3.7% of mean ADR
MAE	0.055 mm/yr	≤ 15% of mean ADR	3.2% of mean ADR
MAPE	4.0%	≤ 10%	Within threshold
Severity-classification accuracy	91.7% (11/12); exact 95% CI: 61.5-99.8%	≥ 85%	One boundary misclassification (Location J)

Note: Continuous validation metrics were calculated from the predicted and observed annual degradation rates for the twelve study locations. The confidence interval for severity-classification accuracy was estimated using the exact Clopper-Pearson binomial method.

To verify the numerical consistency of the reported validation results, the principal performance metrics were recalculated directly from the location-level predicted and observed degradation-rate pairs presented in Table 5. The recalculated values closely matched the rounded values reported in Table 6, providing an internal computational verification of the correlation and prediction-error statistics. This recalculation constitutes a numerical consistency check and should not be interpreted as an independent validation dataset.

Table 7. *Numerical verification of the in-sample validation statistics using the location-level data in Table 5.*

Metric	Value reported in Table 6	Recomputed from Table 5
Pearson correlation, r	0.998	0.9979
Spearman rank correlation, ρ	1.000	1.000
Predictive R^2	0.993	0.9934
RMSE (mm/yr)	0.064	0.0633
MAE (mm/yr)	0.055	0.0542
MAPE (%)	4.0	3.94

Note: Recomputed directly from the twelve predicted and observed degradation-rate pairs reported in Table 5. Differences between the two columns reflect rounding only; the recalculation is an internal numerical verification rather than a separate validation exercise.

The predicted-versus-observed LSDF severity-classification confusion matrix (Table 8) shows one boundary misclassification at Location J, yielding an overall classification accuracy of 91.7% (11/12) with an exact 95% Clopper-Pearson confidence interval of 61.5-99.8%. Observed severity classes were assigned independently from the observed annual degradation rates using the effective-corrosion-rate thresholds specified in Table 4, whereas predicted severity classes were obtained by applying the same effective-corrosion-rate thresholds (Table 4) to the predicted effective corrosion rate, CR_{eff}, rather than directly from the LSDF severity band; this keeps predicted and observed classes on a common corrosion-rate scale. This distinction prevents the observed classification from being defined directly by the LSDF prediction itself.

Location J illustrates the boundary sensitivity of the classification procedure. Its predicted effective corrosion rate of 0.79 mm/yr falls just below the Very Low/Low threshold of

0.8 mm/yr, whereas its observed ADR of 0.84 mm/yr falls just above it, within the Low range of 0.8-1.2 mm/yr. Thus, the single classification disagreement occurs immediately adjacent to a class boundary rather than representing a large discrepancy between predicted and observed degradation behaviour.

Table 8. *Confusion matrix / classification results (actual rows, predicted columns; n=12).*

Actual / Predicted	Critical	High	Moderate	Low	Very Low
Critical	3	0	0	0	0
High	0	3	0	0	0
Moderate	0	0	2	0	0
Low	0	0	0	1	1
Very Low	0	0	0	0	2

Per-class precision, recall and F1, derived arithmetically from Table 8, are reported in Table 9.

Table 9. *Per-class precision, recall and F1-score, derived from the confusion matrix (Table 8).*

LSDF severity class	Precision	Recall	F1
Critical	1.000	1.000	1.000
High	1.000	1.000	1.000
Moderate	1.000	1.000	1.000
Low	1.000	0.500	0.667
Very Low	0.667	1.000	0.800
Macro-average	—	—	0.893

Author-computed from Table 8 using Equations (11)-(14). Balanced accuracy (mean class recall) = 0.900, slightly below the overall (micro-averaged) accuracy of 91.7%; the difference reflects the smaller Low class (n=2) receiving equal weight to the larger classes under macro-averaging.

3.3. Leave-one-location-out Cross-validation

LOLO-CV results (Table 10) show a stable refit k across folds (range 4.710-4.804), indicating that the calibration constant is not unduly sensitive to the removal of any single location. Under LOLO-CV, mean absolute error was 0.062 mm/yr, RMSE was 0.073 mm/yr, and the maximum absolute error was 0.142 mm/yr (Location A). Applying the same effective-corrosion-rate-threshold classification procedure used in Section 3.2 to the LOLO-predicted CR_eff values in Table 10, classification accuracy under LOLO-CV was 91.7% (11/12; exact 95% Clopper-Pearson CI 61.5-99.8%), with Location J whose LOLO-predicted CR_{eff} of 0.792 mm/yr again falls immediately below the 0.8 mm/yr Very Low/Low threshold against an observed ADR of 0.84 mm/yr remaining the sole misclassification, consistent with the in-sample result of Section 3.2. Continuous-error performance nonetheless degrades under cross-validation relative to the in-sample fit (RMSE 0.073 mm/yr versus 0.064 mm/yr; MAE 0.062 mm/yr versus 0.055 mm/yr), consistent with general evidence that apparent (in-sample) and cross-validated performance estimates for small samples should not be conflated [13]. The LOLO RMSE was computed by the authors directly from the twelve absolute errors of Table 10, consistent with the methodology of Section 2.4, which specifies MAE, RMSE, maximum absolute error and classification accuracy as the LOLO summary statistics.

Table 10. Leave-one-location-out cross-validation results.

Location removed	Refit k	Predicted CR_{eff} (mm/yr)	Observed ADR (mm/yr)	Absolute error (mm/yr)
A	4.804	2.902	2.76	0.142
B	4.769	2.583	2.51	0.073
C	4.752	2.706	2.68	0.026
D	4.722	2.368	2.42	0.052
E	4.710	1.989	2.10	0.111
F	4.717	1.867	1.96	0.093
G	4.738	1.708	1.72	0.012
H	4.732	1.564	1.61	0.046
I	4.742	0.901	0.89	0.011
J	4.738	0.792	0.84	0.048
K	4.739	0.605	0.69	0.085
L	4.741	0.500	0.54	0.040

LOLO-CV summary: MAE = 0.062 mm/yr; RMSE = 0.073 mm/yr; maximum absolute error = 0.142 mm/yr; classification accuracy = 91.7% (11/12; exact 95% Clopper-Pearson CI 61.5-99.8%).

3.4. Terrain-specific Validation

Prediction errors were also examined separately by terrain class using the location-level predicted and observed degradation rates presented in Table 5. Because each terrain class contains only four locations, the resulting statistics are interpreted as descriptive diagnostics rather than as statistically conclusive evidence of terrain-specific model performance.

Table 11. Terrain-specific continuous prediction-error metrics derived from the location-level validation data.

Terrain class	Pearson r	RMSE (mm/yr)	MAE (mm/yr)	Mean observed ADR (mm/yr)
Coastal mangrove (A-D)	0.979	0.067	0.058	2.592
Transitional swamp (E-H)	0.994	0.070	0.060	1.848
Inland upland fringe (I-L)	0.983	0.051	0.045	0.740

Terrain-specific statistics were calculated directly from the location-level predicted and observed degradation rates in Table 5. Given the small number of locations within each terrain class (n=4), these results are interpreted descriptively.

3.5. Comparison with a Uniform 36-month Benchmark Schedule

Table 12 compares, location by location, the LSDF-prescribed interval (assigned by the decision matrix of Table 4) against the uniform 36-month static inspection benchmark. The comparison quantifies how the proposed LSDF policy reallocates inspection frequency relative to a uniform benchmark; it is a policy-comparison analysis rather than an independent validation of the LSDF-derived inspection intervals, since the LSDF-prescribed interval is the reference against which the benchmark is scored, not an independently derived requirement. On this basis, the benchmark schedule was less frequent than the LSDF-prescribed interval for all eight Critical/High/Moderate locations (A-H), by 12-30 months depending on location, and more frequent than the LSDF-prescribed interval for all four Very Low-exposure locations (I-L), by 24 months.

Table 12. LSDF-prescribed versus uniform 36-month benchmark inspection intervals, by location.

Location	LSDF-prescribed interval (mo.)	Uniform benchmark (mo.)	Difference from LSDF-prescribed interval (mo.)
A	6	36	+30
B	6	36	+30
C	6	36	+30
D	12	36	+24
E	12	36	+24
F	24	36	+12
G	24	36	+12
H	24	36	+12
I	60	36	−24
J	60	36	−24
K	60	36	−24
L	60	36	−24

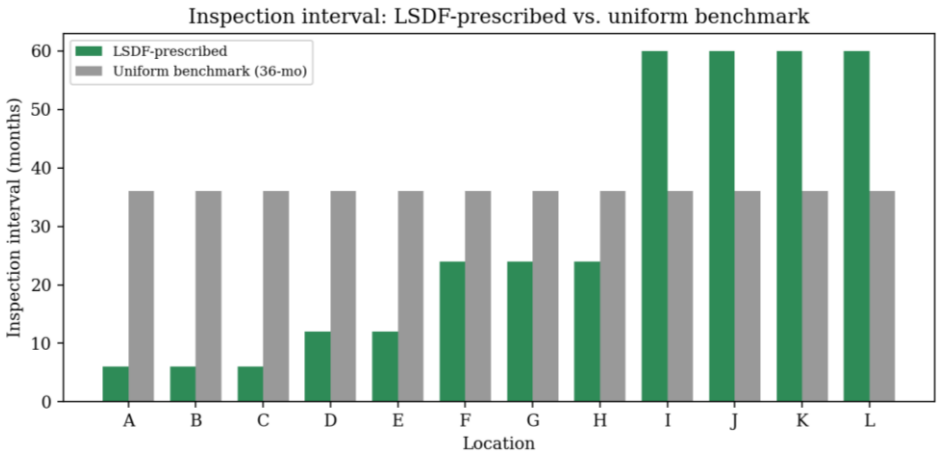


Figure 4. Inspection interval by location: LSDF-prescribed versus uniform 36-month benchmark.

The practically important message is not that the LSDF-adjusted schedule reduces every inspection interval; it reallocates inspection frequency according to location-specific degradation severity. Table 13 quantifies this reallocation: Critical locations are inspected 5.5 times more often than under the uniform benchmark, while Very Low-exposure locations are inspected at the same frequency as before (2 inspections per 5 years under the reconciled event-counting rule), so no reduction in Very Low-exposure inspection burden is claimed relative to that reconciled baseline.

Table 13. Inspection-event comparison: uniform 36-month benchmark versus LSDF-adjusted framework.

Dimension	Uniform benchmark	LSDF-adjusted framework	Outcome
Very Low-exposure inspection frequency	2 inspections / 5 yr	2 inspections / 5 yr	No change (reconciled 5-yr counting rule)
Critical-location inspection	2 inspections / 5 yr	11 inspections / 5 yr	5.5× more frequent at Critical locations

Dimension	Uniform benchmark	LSDF-adjusted framework	Outcome
Total inspection events (5-yr horizon)	24	62	+158.3% (an increase, not a reduction)

Note: Inspection-event counts were calculated consistently for both schedules using the five-year event-counting convention defined in Equation (17).

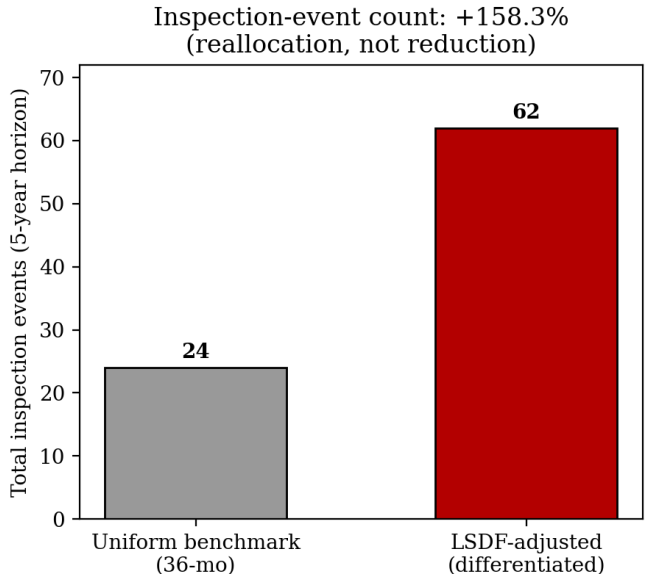


Figure 5. *Total five-year inspection events: uniform benchmark (24) versus LSDF-adjusted (62).*

3.6. Over-scheduling and Under-scheduling Relative to the LSDF Policy

Table 14 reports over-scheduling and under-scheduling relative to the LSDF policy using directly calculated scheduling counts. Because the LSDF schedule defines the reference intervals, these counts are interpreted as scheduling-reallocation measures rather than diagnostic accuracy, false-alarm or miss-rate statistics. Relative to the study-specific LSDF interval policy, the uniform 36-month benchmark schedules inspections less frequently than prescribed for all eight Critical/High/Moderate locations (A-H) and more frequently than prescribed for all four Very Low-exposure locations (I-L): all eight higher-severity locations were under-scheduled relative to the LSDF policy (8/8) and all four Very Low-exposure locations were over-scheduled relative to the LSDF policy (4/4) under the uniform benchmark, whereas the LSDF-adjusted schedule is, by construction, neither over- nor under-scheduled relative to its own policy (0/8 and 0/4).

Table 14. *Locations under-scheduled and over-scheduled relative to the LSDF policy: uniform 36-month benchmark versus LSDF-adjusted framework.*

Scheduling comparison	LSDF-adjusted framework	Uniform 36-month benchmark
Higher-severity locations under-scheduled relative to the LSDF policy (Critical/High/Moderate; A-H)	0/8	8/8
Very Low-exposure locations over-scheduled relative to the LSDF policy (I-L)	0/4	4/4

Note: These counts describe scheduling differences relative to the study-specific LSDF interval policy. They are not interpreted as false-positive, false-negative, false-alarm or diagnostic-accuracy measures because the LSDF schedule itself defines the reference inspection intervals.

3.7. Economic Scope of the Inspection-policy Comparison

The present analysis evaluates inspection scheduling and inspection-event frequency but does not undertake a full economic optimisation. The LSDF-adjusted policy generated 62 scheduled inspection events over the five-year analysis horizon compared with 24 events under the uniform 36-month benchmark, representing an increase of 158.3%. This increase reflects the substantially shorter inspection intervals assigned to locations with higher degradation-exposure severity.

A defensible economic assessment would require location-specific inspection costs, mobilisation and access costs, monitoring costs, failure-consequence estimates, avoided-loss benefits, discount rates and an explicit benefit-timing convention. These inputs were not available for the present twelve-location dataset. Consequently, no NPV, ROI, payback-period

or net cost-saving claim is made. The present results therefore support an inspection-resource reallocation argument rather than an economic-benefit claim: greater inspection effort is directed toward higher-severity locations, while Very Low-exposure locations are inspected less frequently than would be required under the higher-severity schedules.

4. Discussion

4.1. Interpretation of Validation and Comparative-evaluation Results

The results support a specific and bounded conclusion: the comparative analysis demonstrates that incorporating location-specific degradation exposure produces differentiated inspection schedules relative to a uniform static benchmark within the twelve-location sample. The in-sample validation statistics ($r=0.998$, $R^2=0.993$, RMSE=0.064 mm/yr, 91.7% classification accuracy) are strong, and classification accuracy under leave-one-location-out cross-validation was preserved at the same 91.7%; the more conservative indicator of likely out-of-sample performance is instead the LOLO-CV continuous-error metrics (RMSE=0.073 mm/yr, MAE=0.062 mm/yr versus 0.064 and 0.055 mm/yr in-sample), which are reported here precisely so that degradation in fit is not obscured by the more favourable apparent-fit figures. Both sets of figures are legitimate and complementary: the in-sample statistics establish that the fitted relationship describes the twelve-location dataset well, while the cross-validated statistics estimate how that relationship is likely to generalise.

The comparative-evaluation results (Section 3.5) show that the practical value of the LSDF-adjusted schedule lies in reallocating inspection effort, not in reducing it: total inspection events increased by 158.3%, concentrated at Critical- and High-severity locations (Section 3.7). This is consistent with, and does not weaken, the framework's core safety rationale: risk-based inspection is intended to allocate inspection resources according to risk rather than uniformly [1, 2], and eliminating both the over-scheduling of Very Low-exposure assets and the systematic under-scheduling of higher-severity assets relative to the LSDF policy (Table 14) is itself a materially significant integrity outcome, independent of any net cost claim. The present analysis therefore limits its economic scope to inspection-event arithmetic because unit inspection costs, mobilisation costs, monitoring costs, avoided-failure costs, discount rates and benefit timing were unavailable, so a full life-cycle economic model was not developed.

This pattern of a corrosion/risk model whose comparative economic benefit depends on costed avoided-failure and inspection data that were not available for the present dataset which recurs in the broader risk-based maintenance literature: recent corrosion-growth-informed maintenance-decision models for subsea pipelines similarly separate the technical corrosion-progression and severity-classification result from the economic optimisation layer, which requires its own explicit cost inputs [14]. The present paper follows the same discipline by reporting the technical validation and comparative-interval results in full while declining to report an economic figure that cannot be supported by the available data.

4.2. Practical Engineering Significance

The validated LSDF-to-RBI pathway is intended to inform, rather than replace, several established integrity-management activities:

1) RBI inspection prioritisation — ranking assets for inspection scheduling within an API RP 580/581-based programme [1, 2];
2) NDT selection — the decision matrix (Table 4) links LSDF severity class to indicative inspection technique (e.g., ILI/MFL+UT and PAUT at Critical locations versus visual/spot-check UT at Very Low locations);
3) cathodic-protection (CP) review — prioritising CP survey and remediation at high-LSDF, high-salinity/soil-corrosivity locations;
4) corrosion-control intervention — targeting inhibitor, coating or monitoring upgrades where the effective corrosion rate is elevated;
5) pipeline accessibility planning — informing logistics and access planning for locations with elevated accessibility-related exposure scores;
6) MIC surveillance — prioritising microbiological monitoring where MIC activity contributes materially to a location's LSDF;
7) security/vandalism monitoring — directing surveillance and community-engagement resources toward locations with elevated vandalism-frequency exposure; and
8) maintenance-resource allocation — supporting a defensible, auditable basis for allocating limited inspection and maintenance budgets across a heterogeneous asset population, consistent with International Organization for Standardization (ISO) 55001 asset-management requirements [15].

In each case, the LSDF and its derived effective corrosion rate and inspection interval are presented as a decision-support layer complementing API-style RBI and existing fitness-for-service and condition-based assessment practice, not as a replacement for them. Any application of the decision matrix in Table 4 remains subject to engineering review, current asset condition, failure-consequence assessment, inspection effectiveness and applicable regulatory requirements.

4.3. External Validity and Limitations

First, the analysis is based on only twelve locations, and the same location-level dataset informed LSDF construction and internal model evaluation. Calibration/validation role separation and LOLO-CV reduce, but do not eliminate, dependence between model development and evaluation. Second, terrain-

specific validation is limited by the small number of locations within each terrain class (n=4). Third, the study provides internal rather than external validation; broader multi-operator testing across a larger and more heterogeneous asset population is required before predictive performance can be generalised beyond the present dataset.

5. Conclusion

This paper internally validated an LSDF-adjusted inspection pathway that converts an AHP-weighted Location-Specific Degradation Factor into an effective corrosion rate, an LSDF severity classification and a differentiated inspection interval, for twelve Niger Delta pipeline locations. Predicted-versus-observed validation showed strong in-sample agreement ($r=0.998$, $R^2=0.993$, 91.7% classification accuracy), independently cross-checked by the authors; leave-one-location-out cross-validation preserved classification accuracy at 91.7% while giving a more conservative RMSE (0.073 mm/yr versus 0.064 mm/yr in-sample), providing a more defensible estimate of likely out-of-sample performance. Relative to a uniform 36-month static inspection benchmark, the LSDF-adjusted schedule reallocated inspection frequency according to location-specific exposure severity, eliminating documented over-scheduling of Very Low-exposure assets and under-scheduling of higher-severity assets relative to the LSDF policy, but increased total five-year inspection events by approximately 158%. No NPV, ROI or net cost-saving claim is made, since location-specific inspection cost, avoided-failure benefit and discount-rate data were not available for the twelve-location dataset. The framework is proposed as a decision-support layer that reallocates inspection effort according to location-specific degradation exposure within, not instead of, established RBI practice, pending broader multi-operator validation.

Abbreviations

ADR	Annual Degradation Rate
AHP	Analytic Hierarchy Process
API	American Petroleum Institute
CI	Confidence Interval
CO_2	Carbon Dioxide
CP	Cathodic Protection
CR	Consistency Ratio
CR_{base}	Baseline Corrosion Rate
CR_{eff}	Effective Corrosion Rate
ECDA	External Corrosion Direct Assessment
F1	F1-score (Harmonic Mean of Precision and Recall)
FN	False Negative
FP	False Positive
ILI	In-Line Inspection
ISO	International Organization for Standardization
LOLO-CV	Leave-One-Location-Out Cross-Validation
LSDF	Location-Specific Degradation Factor
MAE	Mean Absolute Error
MAPE	Mean Absolute Percentage Error
MFL	Magnetic Flux Leakage
MIC	Microbiologically Influenced Corrosion
NDT	Non-Destructive Testing
NOSDRA	National Oil Spill Detection and Response Agency
NPV	Net Present Value
PAUT	Phased-Array Ultrasonic Testing
RBI	Risk-Based Inspection
RMSE	Root-Mean-Square Error
ROI	Return on Investment
RP	Recommended Practice
TP	True Positive
UT	Ultrasonic Testing

Acknowledgements

The authors thank the expert panel and data sources underlying the LSDF-development analysis.

Author Contributions

Utiri Collins David: Data curation, Formal Analysis, Investigation, Visualization, Writing – original draft

Elizabeth Chinyerem Ndubuisi: Conceptualization, Methodology, Project administration, Supervision, Writing – review & editing

Data Availability Statement

The predicted and observed degradation-rate data, severity-classification results, leave-one-location-out cross-validation results and inspection-schedule comparison underlying this study are available from the corresponding author upon reasonable request.

Conflicts of Interest

The authors declare that they have no known competing financial interests or personal relationships that could have appeared to influence the work reported in this paper.

References

[1] American Petroleum Institute (API). API RP 580: Risk-based Inspection, 4th ed. API. 2023.

[2] American Petroleum Institute (API). API RP 581: Risk-based Inspection Methodology, 4th ed. API. 2025.

[3] Khan, F., Yarveisy, R., Abbassi, R. Risk-based pipeline integrity management: a road map for the resilient pipelines. Journal of Pipeline Science and Engineering. 2021, 1(1), 74-87. https://doi.org/10.1016/j.jpse.2021.02.001

[4] Huang, Y., Qin, G., Yang, M. A risk-based approach to inspection planning for pipelines considering the coupling effect of corrosion and dents. Process Safety and Environmental Protection. 2023, 180, 588-600. https://doi.org/10.1016/j.psep.2023.10.025

[5] Nairametrics. Nigeria recorded over 589 oil spills in 2024, most caused by oil theft. Nairametrics, 17 January 2025 (citing NOSDRA Oil Spill Monitor data).

[6] Ozougwu, P. E., Madu, C. N., Chukwuorji, J. C., Ozougwu, A. O., Ozougwu, S. U. Environmental identities and attitude towards crude oil pipeline vandalism in Niger Delta oil-producing communities. Sustainability. 2023, 15(6), 5610. https://doi.org/10.3390/su15065610

[7] Jacob, J., Varadharajan, R. Robust variance inflation factor: a promising approach for collinearity diagnostics in the presence of outliers. Sankhya B. 2024, 86(2), 845-871. https://doi.org/10.1007/s13571-024-00342-y

[8] Javaherdashti, R. Editorial: Microbiologically influenced corrosion (MIC): its mechanisms, technological, economic, and environmental impacts. Frontiers in Microbiology. 2023, 14, 1249565. https://doi.org/10.3389/fmicb.2023.1249565

[9] Santhosh Kumar, A., Sivakumar, L., Rajadesingu, S., Sathish, S., Malik, T., Parthipan, P. Sustainable corrosion inhibition approaches for the mitigation of microbiologically influenced corrosion—a systematic review. Frontiers in Materials. 2025, 12, 1545245. https://doi.org/10.3389/fmats.2025.1545245

[10] Prokhorov, O., Prokhorov, V., Tevyashev, A., Khussanov, A., Khussanov, Z., Turdybekova, D. A method for importance and risk assessment of main pipeline facilities. Eastern-European Journal of Enterprise Technologies. 2023, 4(3), 33-44. https://doi.org/10.15587/1729-4061.2023.285862

[11] Dong, Z., Zhang, M., Li, W., Wen, F., Dong, G., Zou, L., Zhang, Y. Development of a predictive model for carbon dioxide corrosion rate and severity based on machine learning algorithms. Materials. 2024, 17(16), 4046. https://doi.org/10.3390/ma17164046

[12] Khalaf, A. H., Lin, B., Abdalla, A. N., Han, Z., Xiao, Y., Tang, J. Enhanced prediction of corrosion rates of pipeline steels using simulated annealing-optimized ANFIS models. Results in Engineering. 2024, 24, 102853. https://doi.org/10.1016/j.rineng.2024.102853

[13] Geroldinger, A., Lusa, L., Nold, M., Heinze, G. Leave-one-out cross-validation, penalization, and differential bias of some prediction model performance measures—a simulation study. Diagnostic and Prognostic Research. 2023, 7, 9. https://doi.org/10.1186/s41512-023-00146-0

[14] Li, X., Liu, Y., Han, Z., Chen, G. A risk-based maintenance decision model for subsea pipeline considering pitting corrosion growth. Process Safety and Environmental Protection. 2024, 184, 1306-1317. https://doi.org/10.1016/j.psep.2024.02.072

[15] International Organization for Standardization (ISO). ISO 55001: Asset Management — Management Systems — Requirements. ISO. 2024.